

**Interfacially dominated giant magnetoresistance in Fe/Cr superlattices**J. Santamaria,<sup>1,\*</sup> M.-E. Gomez,<sup>1,†</sup> M.-C. Cyrille,<sup>1,‡</sup> C. Leighton,<sup>1</sup> Kannan M. Krishnan,<sup>2</sup> and Ivan K. Schuller<sup>1</sup><sup>1</sup>*Department of Physics, University of California—San Diego, La Jolla, California 92093-0319*<sup>2</sup>*Materials Sciences Division, National Center for Electron Microscopy, Lawrence Berkeley Laboratory, University of California—Berkeley, Berkeley, California 94720*

(Received 14 August 2001; published 3 December 2001)

We have performed an extensive comparative study of growth, structure, magnetization, and magnetotransport in Fe/Cr superlattices. A simple analysis of the experimental data shows that the giant magnetoresistance originates from interfacial scattering in the Fe/Cr system. The saturation resistivity is determined by the roughness lateral correlation length whereas the giant magnetoresistance is determined by the interface width.

DOI: 10.1103/PhysRevB.65.012412

PACS number(s): 75.70.Cn, 75.70.Pa

Studies of giant magnetoresistance (GMR) in metallic superlattices have produced much new physics since its discovery.<sup>1–3</sup> Most studies of magnetotransport in metallic superlattices are performed with the current parallel to the interfaces [current in the plane (CIP)] geometry. However, the geometry in which the current flows perpendicular to the interfaces [current perpendicular to the plane (CPP)] (Refs. 4–10) is much more amenable to theoretical studies, and has recently produced important applications.<sup>11</sup> To the best of our knowledge there are no experimental studies that connect in a quantitative fashion well-defined structural parameters and magnetotransport. The reasons for this are as follows: CPP measurements are notoriously difficult experimentally, the structural complexity of a superlattice requires detailed-quantitative structural measurements, sample characteristics are delicately dependent on preparation conditions, and the magnetic properties are strikingly affected by small changes in preparation conditions and structural parameters. To address all these issues we have performed a detailed experimental study to investigate the connection between CPP-GMR and structure. To do this we brought together two well-established quantitative structural analysis techniques with a lithography-based CPP measurement technique and magnetization on a large set of samples. We find evidence that in Fe/Cr superlattices both the CPP resistivity and the CPP-GMR originate mainly from the interfaces. These results provide well-defined quantitative results that should be key ingredients in theories dealing with GMR in metallic superlattices.

Studies of transport in metallic superlattices are affected by many inherent complexities of the material. Many possible complications arise in these types of artificial materials: a) interfacial roughness and/or interdiffusion at various lateral length scales,<sup>12–14</sup> (b) bulk defects, (c) structural changes as a function of individual layer and/or overall thickness, (d) different length scales affecting the structure, magnetism, and transport, and (e) differences in the magnetotransport along the different directions in the superlattices. Moreover, theoretical treatments of the problem are much more amenable if the current flow is perpendicular to the interfaces of the layers (CPP). It is, therefore, desirable to have a study in which the CPP-GMR is directly related to structural parameters independently measured using quantitative structural probes. The quantitative determination of all

structural parameters in a superlattice is rather difficult since different techniques give information with varying accuracy along different directions (perpendicular or parallel to the interfaces). In order to obtain a quantitative description of the superlattice it is useful to cross correlate various measurement techniques on samples made under different conditions. The measurement of the magnetoresistance is also complicated by the fact that it is desirable to measure independently the resistivity and the magnetoresistance. The reason for this is that these two quantities may be affected in different ways by structural parameters and, therefore, a measurement solely of the ratio of the two quantities may not be sufficient. Moreover, the GMR depends also on the degree of antiferromagnetic (AF) alignment in the superlattice and, therefore, measurements of the magnetization are also a key ingredient in order to obtain a clear cut answer.

A key issue in the mechanism of GMR is the relative importance of bulk and interfacial scattering. This is particularly difficult to clarify since in many cases both the bulk and interfacial scattering are affected when layer or overall thicknesses of the superlattice are varied. Moreover, in the CPP measurements the roughness and interdiffusion are also affected by the initial roughness of the electrodes underlying the sample. Due to this, whether the GMR is mostly interfacial or bulk in origin is quite controversial. Measurements as a function of layer thickness, analyzed within a particular model have claimed that the GMR originates from the bulk and that interfacial roughness does not play a crucial role.<sup>15</sup> Other measurements in which the interfaces were modified by the addition of small amounts of interfacial impurities, claim that the interfacial scattering plays a dominant role.<sup>16</sup> It may even be possible that the exact mechanism is materials system dependent. It seems that no experiments are available where the role played by “long-wavelength” roughness (larger than atomic) was investigated.

Here we have tackled this problem in a comprehensive fashion. We have made two different types of superlattices by sputtering, where we vary: a) the number of bilayers, and b) sputtering pressure with a fixed number of bilayers. We have characterized the structure of the superlattices using quantitative x-ray diffraction and quantitative energy-filtered transmission electron microscopy (EFTEM) spectra. We measured the magnetization in order to obtain a quantitative measure of the antiferromagnetically aligned fraction. This is

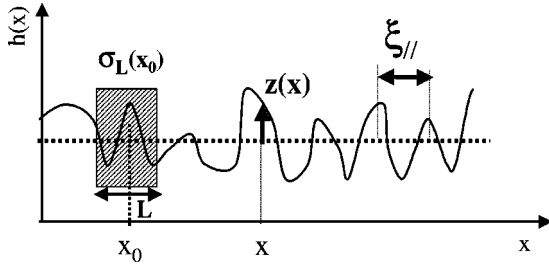


FIG. 1. Sketch of a rough surface with the various characteristic length scales. The dotted line is the averaged height with respect to the height deviation  $z$ . The dashed window of size  $L$  is the region over which the standard deviation of heights is calculated to obtain the size-dependent roughness. The lateral correlation length  $\xi_{\parallel}$  is roughly the distance between surface “bumps.”

particularly important when roughness is present because it can cause local changes of the coupling or magnetic shorts. In addition we have measured independently the CPP resistivity and magnetoresistance in photolithographically prepared samples of a well-defined geometry. We spent considerable effort to ascertain that the measurement of the resistivity is free of nontrivial measurement artifacts<sup>16,17</sup> that are particularly important for CPP measurements.

To avoid many of these difficulties, in the present experiment we have fixed the individual layer thicknesses of Fe(30 Å)/Cr(12 Å) (this Cr thickness corresponds to a peak in AF coupling), and varied other structural parameters such as the overall thickness (i.e., number of bilayers  $N$ ) and the sputtering pressure  $P$ . The conclusions obtained here are based on a comprehensive analysis of more than 40 samples. Nb-(Fe/Cr) $_N$ -Nb multilayers were prepared using high-rate magnetron sputtering with the detailed preparation conditions described elsewhere.<sup>17,18</sup> We have conducted this experiment with two different sets of samples: set *A* consists of fixed-low-pressure samples (5 mTorr) in which the number of bilayers has been changed between 17 and 40; and set *B* with samples with a constant number of 20 bilayers, grown at pressures between 5 and 10 mTorr. Superconducting Nb electrodes serve as electrodes for the CPP measurements. A structural characterization was performed using quantitative analysis of specular x-ray diffraction (XRD) using the SUPREX (Ref. 19) model and quantitative EFTEM. Magnetization measurements were performed using a superconducting quantum interference device magnetometer. The magnetotransport measurements were performed in photolithographically prepared samples of well-defined geometry. This allows independent measurement of the resistivity and the magnetoresistance. The details of all measurement and preparation techniques were described elsewhere together with a detailed discussion of possible measurement artifacts.<sup>17,18</sup>

To quantify the roughness we describe the single-interface profile [ $h(x)$ ] in terms of the height deviation [ $z(x)$ ] with respect to an averaged value [ $\langle h(x) \rangle$ ] (see Fig. 1). The rms roughness (also termed interface width) for an in-plane system of size  $L$  is defined as  $\sigma(L) = [\langle |z(x) - z_{av}(L)|^2 \rangle_L]^{1/2}$  where  $z_{av}(L)$  is  $z(x)$  averaged over  $L$ , and the average is done over all points  $x$  within  $L$ .

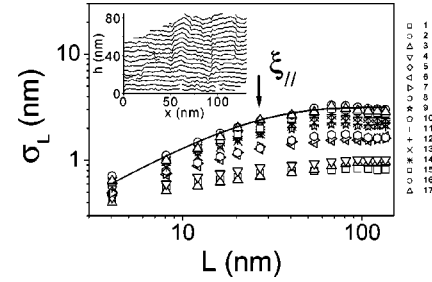


FIG. 2. Size-dependent roughness for the individual bilayers of a 20-bilayer Fe/Cr superlattice grown at 8 mTorr. Roughness increases from lower to upper bilayer index (bottom to top in the figure). The key specifies the bilayer index from bottom to top. The lateral correlation length  $\xi_{\parallel}$  is extracted by fitting the roughness for each bilayer to  $\sigma(L) = \sigma_{sat} [1 - \exp(-L/\xi_{\parallel})^{2\alpha}]^{1/2}$  with  $\alpha = 0.7 \pm 0.05$  (see line). Inset: digitized Cr EFTEM profile of the same sample.

The inset of Fig. 2 shows a digitized EFTEM map using the Cr  $L_{3,2}$  edge of a 20 bilayers Fe/Cr superlattice grown at 8 mTorr. Similar maps were also obtained using the Fe  $L_{3,2}$  edge but no substantial difference was observed between the Fe and Cr profiles. Hence, a representative profile of the layers constructed with the maxima of the intensities of the Cr  $L_{3,2}$  edge is shown. These profiles show the bilayer modulation in cross section and can be assumed to represent the bilayer roughness, i.e., we do not account for the difference in roughness between both layers. A substantial replication of the long-scale roughness can be readily observed (correlated roughness). The study of the lateral correlation of the roughness is done locally by averaging the roughness over different window sizes.<sup>19</sup> For each bilayer, the local roughness for window size  $L$ , at a point  $x_0$ , is obtained as  $\sigma_L(x_0) = [\langle |z(x) - z_{av}(L)|^2 \rangle_L]^{1/2}$  averaging over  $L$ . The size-dependent roughness  $\sigma(L)$  is then obtained averaging over each bilayer as  $\sigma(L) = \langle \sigma_L(x_0) \rangle_x$  (see Fig. 1). Figure 2 shows the size ( $L$ ) dependence of the roughness of an 8 mTorr sample for several bilayers. For each interface, roughness increases as a power law and then saturates (roughness cutoff). The characteristic length scale over which roughness saturates is the lateral correlation length ( $\xi_{\parallel}$ ), i.e., the distance over which interface heights “know about each other.” Many numerical simulations have shown that this corresponds to the average distance between surface “bumps,” and in polycrystalline samples  $\xi_{\parallel}$  coincides with grain size.<sup>20</sup> The correlation length is extracted for each bilayer, fitting the lateral dependence of the roughness to  $\sigma(L) = \sigma_{sat} [1 - \exp(-L/\xi_{\parallel})^{2\alpha}]^{1/2}$  with  $\alpha = 0.7 \pm 0.05$  (line in the figure). We note that the roughness length scale in all samples (10–20 nm) is comparable or larger than that of the cross-section thickness used in the EFTEM measurements. Consequently this evaluation is free of artifacts due to the projection of the two-dimensional (2D) roughness pattern on the 1D bilayer profiles. It is also worth noting that the lateral correlation length, in the range 10–20 nm, obtained here is in agreement with previous reports on similar samples using diffuse x-ray scattering.<sup>21,22</sup>

Specular low-angle XRD patterns were refined using the SUPREX software<sup>19</sup> using a model in which roughness in-

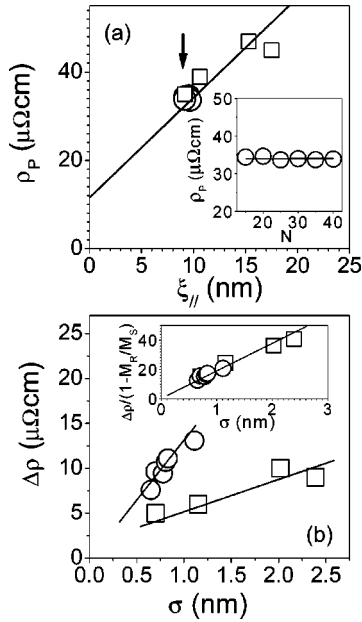


FIG. 3. (a) Saturation resistivity  $\rho_P$  as a function of roughness lateral correlation length  $\xi_{||}$  for set A (circles) and set B (squares). Set A shows almost constant  $\xi_{||}$  values and six data points are overlapping (marked with arrow). For set B (squares)  $\xi_{||}$  increases with pressure. Inset: saturation resistivity vs the number of bilayers for set A. (b)  $\Delta\rho$  as a function of roughness for set A (circles) and set B (squares). Inset:  $\Delta\rho$  as a function of roughness corrected for the AF-aligned fraction. The AF-aligned fraction  $1 - M_R/M_S$  was 0.6 for set A samples, and  $1 - M_R/M_S \approx 0.3$  for set B.

increases cumulatively as a power law of the bilayer index.<sup>17,18</sup> The roughness values obtained from x-ray fitting were in very good agreement (within 10%) with the averaged value of the roughness at saturation obtained from EFTEM.

Structurally, the two sets show a markedly different behavior. For set A, the roughness lateral correlation length ( $\xi_{||}$ ) is independent of bilayer index (or on the number of bilayers), i.e., constant at a value of 10 nm. For set B,  $\xi_{||}$  increased with the number of bilayers and with pressure, attaining a value close to 20 nm for the 10 mTorr sample. The roughness increased with the bilayer index in both sets of samples and also with pressure in set B. The interface width (hereafter referred as “roughness”) at saturation averaged over the different bilayers was in the range 0.5–1 nm for set A, and in the range 0.7–2.4 nm for set B. The level of AF alignment was also different for both kinds of samples: while set A showed an almost constant AF aligned fraction  $1 - M_R/M_S \approx 0.6$ , in set B it attained values close to 0.3, also changing only slightly from sample to sample.<sup>17,18</sup>

As far as the giant magnetoresistance measurements are concerned, set A showed a saturation resistivity  $\rho_P$  independent of the number of bilayers [see inset of Fig. 3(a) and circles in main panel], while it increased with pressure for set B [see squares in Fig. 3(a)]. The roughness increased smoothly with bilayer index, and also with pressure, as stated above. We have found that the saturation resistivity scales with the roughness lateral correlation length ( $\xi_{||}$ ) as illustrated in Fig. 3(a). It is worth noting that set A, with constant  $\xi_{||}$ , also shows constant  $\rho_P$  (open circles in Fig. 3(a)).  $\Delta\rho$

(defined as  $\rho_{AP} - \rho_P$ , with  $\rho_{AP}$  being the zero-field resistivity) increased with roughness for both sets of samples. This roughness value was obtained averaging the saturation values obtained by EFTEM over the different bilayers, and was in very good agreement with the roughness values obtained from low-angle x-ray fitting. The main panel of Fig. 3(b) displays  $\Delta\rho$  for both sets of samples showing clear dependences of GMR with interface roughness. Note that data points from different sets fall into straight lines extrapolating close to zero. It seems that the slope is determined by the degree of ferromagnetic alignment: set A with  $1 - M_R/M_S \approx 0.6$  has larger slope than set B with  $1 - M_R/M_S \approx 0.3$ . Interestingly enough, if  $\Delta\rho$  is corrected for the AF-aligned fraction for both sets of samples dividing by  $1 - M_R/M_S$ , all data points fall into a straight line [see inset of Fig. 3(b)]. This suggests not only a clear dependence of GMR with interface roughness, but also, since this line extrapolates through zero, that roughness is a key ingredient of GMR. It is important to remark that this correction assumes that the main contribution to GMR comes from the AF-aligned portion of the sample. Although this is probably the case in the strong coupling limit of thin Cr layers (like ours), it is worth noting that significant GMR is known to originate from randomly oriented magnetization in weakly coupled layers with thicker nonmagnetic spacers (5–6 nm).<sup>23</sup> Additionally this correction also does not account for possible inhomogeneities in the current distribution due to the lower resistance ferromagnetically aligned portions of the sample.<sup>24</sup>

We have found a clear dependence of resistivity and GMR with long length-scale (10–20 nm) roughness. This result should provide a feedback for theoretical calculations assuming perfect layers.<sup>25</sup> A long-scale roughness may be relevant not only for its contribution to scattering, but also for its influence on the magnetic properties at the interfaces. In fact it has been previously shown from structural probes that magnetic roughness follows the long scale interface roughness.<sup>26–28</sup> It is possible that the roughness lateral correlation length is limited by grain size, which is determined by differences in the growth mechanism at high and low pressures.<sup>29</sup> However, this does not necessarily imply that the saturation resistivity originates from bulk scattering. It is known that the resistivity of individual Fe and Cr layers is in the range 5–15  $\mu\Omega$  cm. These values are significantly smaller than the saturation resistivities of our samples (in the range 35–55  $\mu\Omega$  cm), clearly pointing to the interfacial origin of the saturation resistivity.

The fact that both  $\Delta\rho$  and  $\rho$  are determined by interface morphology ( $\Delta\rho$  by interface width and  $\rho$  by  $\xi_{||}$ ) provides an explanation for the CIP magnetoresistance (with a reduced interface contribution) being smaller than the CPP in Fe/Cr superlattices. This is in agreement with previous theoretical studies<sup>30</sup> that propose waveguiding through the paramagnetic layer as a source of reduced GMR in the CIP configuration. In addition, it is worthwhile noting that both roughness parameters affect differently the ratio  $\Delta\rho/\rho$ , customarily used to describe GMR.

In summary, a detailed comparison of structure, magne-

tism, and transport shows that in Fe/Cr superlattices the resistivity is mostly dominated by the roughness lateral correlation length, whereas the magnetoresistance is determined by interface width in the Fe/Cr system. These results should provide the quantitative connection between structural measurements and transport for the development of a quantitative theory of GMR.

The authors thank S. Bader, J. Bass, G. Bauer, A. Fert, E. Fullerton, B. J. Hickey, P. Levy, A. M. Llois, and M. Weissman for their fruitful comments. This work was supported by the US Department of Energy and the New del Amo Program. J.S. thanks the Fundacion Jaime del Amo and Fundacion Flores Valles for its support. M.E. Gomez thanks Universidad del Valle and COLCIENCIAS.

\*On leave from U. Complutense, 28040 Madrid, Spain. Email address: jacsan.eucmax.sim.ucm.es

†On leave from Universidad del Valle, A.A.25360 Cali, Colombia.

‡Present address: IBM Almaden.

<sup>1</sup>P. M. Levy, *Solid State Phys.* **47**, 367 (1994), and references therein.

<sup>2</sup>M. A. M. Gijs and G. E. W. Bauer, *Adv. Phys.* **46**, 285 (1997), and references therein.

<sup>3</sup>A. Barthelemy, A. Fert, and F. Petroff, in *Handbook of Magnetism*, edited by K. H. J. Buschow (Elsevier, New York, 1999), Vol. 12, and references therein.

<sup>4</sup>W. P. Pratt Jr., S.-F. Lee, J. M. Slaughter, R. Loloee, P. A. Schroeder, and J. Bass, *Phys. Rev. Lett.* **66**, 3060 (1991).

<sup>5</sup>M. A. M. Gijs, S. K. J. Lenczowski, and J. B. Giesbers, *Phys. Rev. Lett.* **70**, 3343 (1993).

<sup>6</sup>M. A. M. Gijs, M. T. Johnson, A. Reinders, P. E. Huisman, R. J. M. van de Veerdonk, S. K. J. Lenczowski, and R. M. J. van Ganswinkel, *Appl. Phys. Lett.* **66**, 1839 (1995).

<sup>7</sup>T. Ono and T. Shinjo, *J. Phys. Soc. Jpn.* **64**, 363 (1995).

<sup>8</sup>L. Piraux, J. M. George, J. F. Despres, C. Leroy, E. Ferain, R. Legras, K. Ounadjela, and A. Fert, *Appl. Phys. Lett.* **65**, 2484 (1994).

<sup>9</sup>A. Blondel, J. P. Meier, B. Doudin, and J. Ph. Ansermet, *Appl. Phys. Lett.* **65**, 3019 (1994).

<sup>10</sup>K. Liu, K. Nagodawithana, P. C. Searson, and C. L. Chien, *Phys. Rev. B* **51**, 7381 (1995).

<sup>11</sup>J.-G. Zhu, Y. Zheng, and G. A. Prinz, *J. Appl. Phys.* **87**, 6668 (2000).

<sup>12</sup>E. E. Fullerton, D. M. Kelly, J. Guimpel, I. K. Schuller, and Y. Bruynseraede, *Phys. Rev. Lett.* **68**, 859 (1992).

<sup>13</sup>J. M. Colino, I. K. Schuller, V. Korenivski, and K. V. Rao, *Phys. Rev. B* **54**, 13 030 (1996).

<sup>14</sup>M. Velez and I. K. Schuller, *J. Magn. Magn. Mater.* **184**, 275 (1998).

<sup>15</sup>J. E. Mattson, M. E. Brubaker, C. H. Sowers, M. Conover, Z. Qiu, and S. D. Bader, *Phys. Rev. B* **44**, 9378 (1991); Z. Q. Qiu, J. E. Mattson, C. H. Sowers, U. Welp, S. D. Bader, H. Tang, and J. C. Walker, *ibid.* **45**, 2252 (1992).

<sup>16</sup>S. S. P. Parkin, *Phys. Rev. Lett.* **71**, 1641 (1993).

<sup>17</sup>M. C. Cyrille, S. Kim, M. E. Gomez, J. Santamaria, K. M. Krishnan, and I. K. Schuller, *Phys. Rev. B* **62**, 3361 (2000).

<sup>18</sup>M. C. Cyrille, S. Kim, M. E. Gomez, J. Santamaria, C. Leighton, K. M. Krishnan, and I. K. Schuller, *Phys. Rev. B* **62**, 15 079 (2000).

<sup>19</sup>I. K. Schuller, *Phys. Rev. Lett.* **44**, 1597 (1980); W. Sevenhans, M. Gijs, Y. Bruynseraede, H. Homma, and I. K. Schuller, *Phys. Rev. B* **34**, 5955 (1986); E. E. Fullerton, I. K. Schuller, H. Vanderstraeten, and Y. Bruynseraede, *ibid.* **45**, 9292 (1992); D. M. Kelly, E. E. Fullerton, J. Santamaria, and I. K. Schuller, *Scr. Metall. Mater.* **33**, 1603 (1995).

<sup>20</sup>A. L. Barabasi and H. E. Stanley, in *Fractal Concepts in Surface Growth* (Cambridge University Press, Cambridge, 1995).

<sup>21</sup>R. Schad, P. Belien, G. Verbanck, C. D. Potter, H. Fischer, S. Lefebvre, M. Bessiere, V. V. Moshchalkov, and Y. Bruynseraede, *Phys. Rev. B* **57**, 13 692 (1998).

<sup>22</sup>R. Schad, P. Belien, G. Verbanck, V. V. Moshchalkov, Y. Bruynseraede, H. E. Fischer, S. Lefebvre, and M. Bessiere, *Phys. Rev. B* **59**, 1242 (1999).

<sup>23</sup>J. Bass and W. P. Pratt, Jr., *J. Magn. Magn. Mater.* **200**, 274 (1999); J. A. Borchers, J. A. Dura, J. Unguris, D. Tulchinsky, M. H. Kelley, C. F. Majkrzak, S. Y. Hsu, R. Loloee, W. P. Pratt, Jr., and J. Bass, *Phys. Rev. Lett.* **82**, 2796 (1999).

<sup>24</sup>P. M. Levy (private communication).

<sup>25</sup>P. Weinberger, *J. Phys.: Condens. Matter* **8**, 7677 (1996); A. M. Llois and M. Weissman (private communication); P. Zahn *et al.*, *Phys. Rev. Lett.* **80**, 4309 (1998); **75**, 2996 (1995).

<sup>26</sup>J. W. Cable, M. R. Khan, G. P. Felcher, and I. K. Schuller, *Phys. Rev. B* **34**, 1643 (1986).

<sup>27</sup>M. J. Pechan, J. M. Ancher, D. M. Kelly, C. F. Majkrzak, and I. K. Schuller, *J. Appl. Phys.* **75**, 6178 (1994).

<sup>28</sup>J. F. Mac Kay, C. Teichert, D. E. Savage, and M. G. Lagally, *Phys. Rev. Lett.* **77**, 3925 (1996).

<sup>29</sup>E. E. Fullerton, J. Pearson, C. H. Sowers, S. D. Bader, X. Z. Wu, and S. K. Sinha, *Phys. Rev. B* **48**, 17 432 (1993).

<sup>30</sup>W. H. Butler, X. G. Zhang, D. M. C. Nicholson, T. C. Schulthess, and J. M. MacLaren, *Phys. Rev. Lett.* **76**, 3216 (1996); I. Mertig, *J. Appl. Phys.* **79**, 5276 (1996).